Enhancement of Nitriding Rate in SUS304 Austenitic Stainless Steel under Gas Nitriding

K. Gemma and M. Kawakami
Department of Metallurgical Engineering, Faculty of Engineering, Tokai University, Kitakaname 1117 Hiratsuka Kanagawa 259–12, Japan

CONTENTS

ABSTRACT

Austenitic stainless steels show the following irregularities in nitriding behaviour: (1) sudden decrease of nitriding rate at about 873°K; (2) remarkable acceleration of the rate in the temperature range 723 to 873°K; (3) discontinuity of the rate at about 723°K and (4) decrease of temperature dependence of the rate below approximately 723°K. Constants of the growth rate of the layer in nitrided SUS304 austenitic stainless steel are approximately 100 times larger than the diffusion coefficients of nitrogen in γ-iron calculated from the frequency factor and the generally recognised activation energy. In this paper, this acceleration of nitrogen diffusion in SUS304 stainless steel under gas nitriding is mainly discussed in terms of the step rule concept for the precipitation of chromium nitrides (Cr_2N and CrN) in the solid phase with the free energy-temperature diagram of these nitrides. A kinetics model is presented in an attempt to understand nitrogen diffusion in the steel. The phenomenon of the discontinuity of the rate [case (3) above] is discussed in connection with the understanding of the enhancement of the nitriding.

1. INTRODUCTION

Since high chromium alloy steels and stainless steels were first nitrided by Jones /1/, various nitriding methods have been tried. Today, some processes are established and applied in industry, e.g. plasma nitriding and oxinitriding. With regard to the abnormalities of nitriding rate in austenitic stainless steels, Lebrun, Michel and Gantois /2/ were the first to discover the sudden decrease of the rate at about 873°K, a fact later confirmed by Edenhofer /3/. They attributed this phenomenon to a γ–α transformation in the nitrided layer, but Billon and Hendry /4/ postulated that the remarkably high nitriding rate in AISI316 austenitic stainless steel was a result of microcracks formed in the nitrided layer. The present authors have recently reported /5/ new phenomena in the gas nitriding of SUS304 stainless steel; namely, the discontinuity of nitriding rate in the temperature range 693°–733°K and the decrease of temperature dependence of the rate below these temperatures and it was shown that a sudden decrease in the nitriding rate takes place as a result of a termination of the acceleration of the nitriding rate. On the other hand, it has been found that a nitrided layer formed in Invar alloy plated with an Fe–Cr–Ni ternary alloy grows thicker than that formed in the non-plated alloy /6/.

A typical behaviour in the growth of a nitrided layer on SUS304 stainless steel is shown in Fig. 1. The experimental plots in the figure were obtained in this work. The dotted curve indicates the penetration depth of nitrogen calculated from the data of frequency factor (D_0 = 0.91 cm·s^{-1}) and activation energy (Q = 168.5 kJ·mol^{-1}) for the diffusion of nitrogen in γ-iron presented by Grieveson and Turkdogan /7/. All the irregularities mentioned above are shown in Fig. 1 marked (1)–(4). At this time, clearly, a new representation for the general understanding of these phenomena is required because prior hypotheses cannot satisfactorily explain all the irregularities contained in the above cases (3) and (4).

When an Fe–Ni–Cr alloy steel, for example SUS304 stainless steel, is nitrided, it is generally considered that Cr atoms in the alloy as a solute combine with

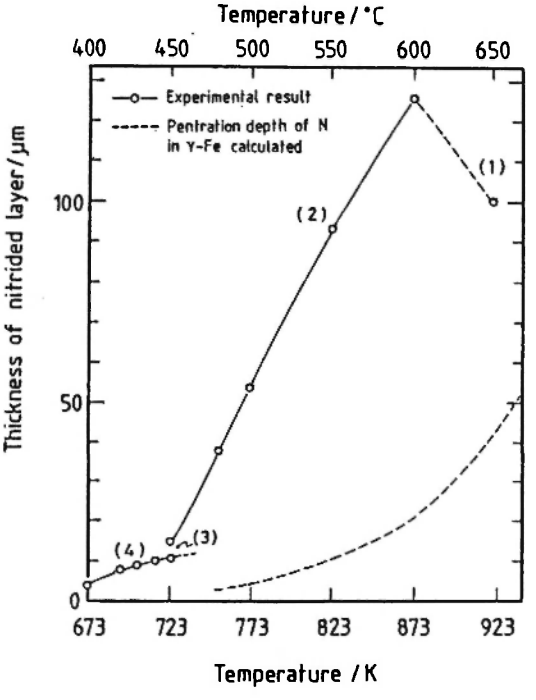

Fig. 1. Thickness of nitrided layer vs temperature for SUS304 stainless steel nitrided in ammonia gas in the temperature range 673°–923°K for 25.2 ks. A dotted curve shows a penetration depth of nitrogen in γ-iron calculated from the frequency factor (D_0 = 0.91 cm^2·s^{-1}) and the activation energy of diffusion (Q = 40260 cal·mol^{-1}) presented by Greaveson and Turkdogan /7/.
(1) a sudden decrease, (2) enhancement, (3) discontinuity and (4) decrease of temperature dependence in the growth of nitrided layer.

nitrogen diffusing from the alloy surface and form chromium nitrides (Cr_2N, CrN or the both). In this case, a free energy-temperature diagram is available for a thermodynamical consideration of the formation of these nitrides in alloys. On the other hand, the conception of "Stufenregel" for precipitation in the solid state /8/ and crystallographical coherency between the precipitates and the parent phase must be considered at the same time.

SUS304 stainless steel (solution treated) was nitrided in ammonia gas for various periods of time at various temperatures. In this paper, the kinetics and the mechanism on the enhancement of the nitriding in SUS304 stainless steel are mainly discussed from the results obtained by means of optical microscopy, X-ray diffractometry and thermogravimetry. In particular, a kinetics model is presented for an understanding of the nitriding rate enhancement in the austenitic stainless steels.

2. EXPERIMENTAL METHODS

SUS304 stainless steels used were a solid solution plate specimen of corrosion tested SUS304 (304–78) of 2 mm thickness supplied by Japan Stainless Association and an industrial grade foil specimen of 15 μm thickness. The chemical composition of the plate specimen is contained in Table 1. Both of the dimensions, 10 mm by 20 mm approximately, were nitrided within the temperature range 673°–923°K for 23.4–32.4 ks in ammonia gas. There was a pretreatment with ammonium chloride vapour for the surface activation of the alloy using a quartz tube 40 mm in diameter fitted in a vertical furnace. After nitriding for a specified time, the specimens were cooled by quenching in a 10% sodium hydroxide solution. The furnace temperature was controlled by an automatic thermo-controller. The temperature of the specimens was measured using a calibrated chromel-alumel thermocouple placed beside it. Before nitriding, the plate specimen was cleaned with fine emery paper and degreased by wiping, dipping in trichloroethane and vapour washing. Finally, it was stored in a desiccator and, just before the nitriding, an ultrasonic treatment in acetone was carried out. The foil specimen was degreased in the same manner, although the emery cleaning was omitted. After nitriding, the cross section of the specimens were treated metallographically and observed with an optical microscope (a marble reagent was used as etchant). The surface of the nitrided plates and planes in the nitrided layer were electrolytically polished in sodium hydroxide-phosphoric acid and were analysed by X-ray diffractometry. The foil specimens were fully nitrided at 673°K and 743°K and examined thermogravimetrically. Also, desorption gas from these specimens at elevated temperatures was analysed by gas chromatography. The residues of these specimens after the thermogravimetric analysis were analysed by X-ray diffractometry.

TABLE 1
Chemical analysis of SUS304 stainless steel used (mass %)

C	Si	Mn	P	S	Ni	Cr	Mo	Cu
0.066	0.56	0.82	0.029	0.002	8.75	18.27	0.14	0.14

3. EXPERIMENTAL RESULTS

3.1. Optical Microstructure and X-ray Diffraction

Optical microstructures of nitrided SUS304 stainless steel are shown in Fig. 2 (a) – (f). The micrographs show nitrided layers formed at (a) 693°K, (b) 753°K, (c) 773°K, (d) 823°K, (e) 873°K and (f) 923°K for 25.2 ks, respectively. These micrographs are selected conveniently to make a comparison with Fig. 1. Nitrided layer (a) is a typical structure formed in the stage where the nitriding rate decreases with a rise in temperature, as illustrated in Fig. 1, and there is no enhancement of the nitriding rate. Nitrided layers (b), (c) and (d) are also typical structures formed in the temperature range where the nitriding rate is enhanced. A characteristic structure difference is clearly apparent between micrographs (a) and (b), namely, whether precipitation has taken place in the layer or not. In micrograph (b), the microstructure of the nitrided layer consists of a whitish phase with some blackish precipitates. This whitish phase seems the same as that forming the layer of micrograph (a). The precipitates increase rapidly with temperature rise whereas the whitish phase decreases. In micrograph (c), a few islands of whitish phase remain just under the surface of the nitrided layer and in micrographs (d) and (e), the whitish phase is hardly visible at all by optical microscopy. In micrograph (f), it can be clearly observed that the nitrided layer formed at 923°K is thinner than the layer formed at 873°K as shown in micrograph (e). These phenomena are of interest to many investigators.

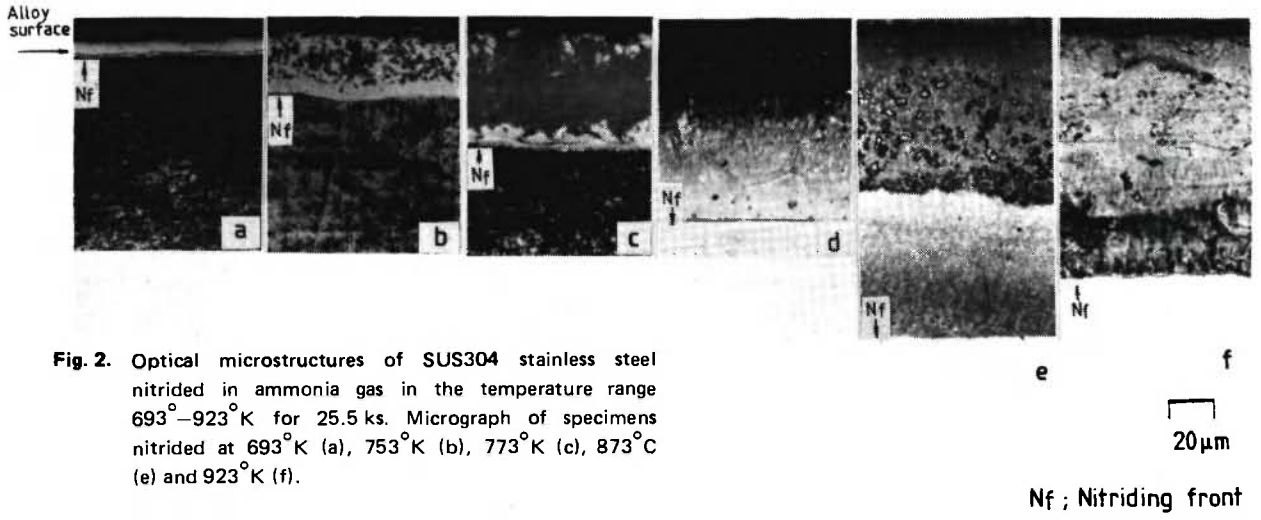

Fig. 2. Optical microstructures of SUS304 stainless steel nitrided in ammonia gas in the temperature range 693°–923°K for 25.5 ks. Micrograph of specimens nitrided at 693°K (a), 753°K (b), 773°K (c), 873°C (e) and 923°K (f).

The above observations indicate that the enhancement of the nitriding rate begins with the commencement of the precipitation in the nitrided layer in the temperature range 693–733°K. It is clear that the discontinuity of the nitriding rate shown in Fig. 1 is caused by this phenomenon but there is another more basic factor; the tendency of chromium nitrides to form in the alloy since the free energy as a function of temperature of formation of these nitrides intersects at approximately 703°K on the free energy-temperature diagram /7/. This will be discussed later.

Some X-ray diffraction analysis of SUS304 stainless steel surfaces nitrided over a low temperature range have been reported /9, 10/. Typical X-ray diffraction patterns obtained from the nitrided surfaces, abraded softly on polishing cloth with 0.03 μm alumina powder, are represented for an understanding of these phenomena in Fig. 3 (a)–(c) /5/. There are austenite, CrN and γ'-Fe_4N detected by collation from ASTM cards with an unknown phase marked $\gamma_{SN1\text{-}5}$, called γ_{SN}-phase in this paper hereafter. Fig. 3 is interesting for two reasons. Firstly, the appearance of CrN and γ'-Fe_4N at temperatures above 753°K; secondly, the shift of some diffraction peaks, for example those of γ_{SN1} and γ_{SN3}, towards low angle positions with rising temperature. Above 773°K, all the peaks of γ_{SN} are fixed, each position and the peak of γ_{SN2} disappear from the diffraction patterns. The first phenomenon suggests that the precipitates in the whitish phase are CrN and γ'-Fe_4N [or γ'-$(Fe,Ni)_4N$ in actuality]. The second indicates that the lattice parameter of the γ_{SN}-phase expands gradually during nitriding with the absorption of a large quantity of nitrogen as temperature rises and, also, that the phase has a fixed crystal structure. Indices of the diffraction pattern of the specimen nitrided at 753°K, Fig. 3 (b), indicate an fcc structure with a lattice parameter of approximately 0.406 nm /5/. The shift of this peak position has been observed and reported in SUS304 stainless steel nitrided by ion nitriding by some investigators /9, 10/, but there is no absolute agreement concerning the formation of the γ_{SN}-phase between them and the authors of this paper and prior /5/. Divisional planes at intervals of 10 μm exposed by electrolytic polishing of the nitrided layer of SUS304 stainless steel nitrided at 873°K for 10.8 ks, were examined by X-ray diffractometer. A change of lattice parameter of austenite formed in this nitrided layer is summarized separately in Table 2 for each divided plane. Table 2 shows clearly that the austenite formed just under the surface is supersaturated with nitrogen and that the existence of a concentration gradient of nitrogen in the nitrided layer is apparent from the lattice parameters measured. Nitrogen contents in the austenites were estimated from the relation between lattice parameter and nitrogen content shown in Fig. 4.

The results obtained from optical microscopy and X-ray diffractometry reveal evidently that the peaks of γ_{SN}-phase in the diffraction patterns are diffracted from the whitish phase observed in the previous micrographs. Accordance in temperature between the discontinuity of the nitriding rate in Fig. 1 and the appearance of the precipitates in Fig. 2 suggests that the precipitation of the γ_{SN}-phase triggers the enhancement of the nitriding in the steel.

When the lattice parameter of the γ_{SN}-phase formed at 753°K is plotted in the diagram of lattice parameter

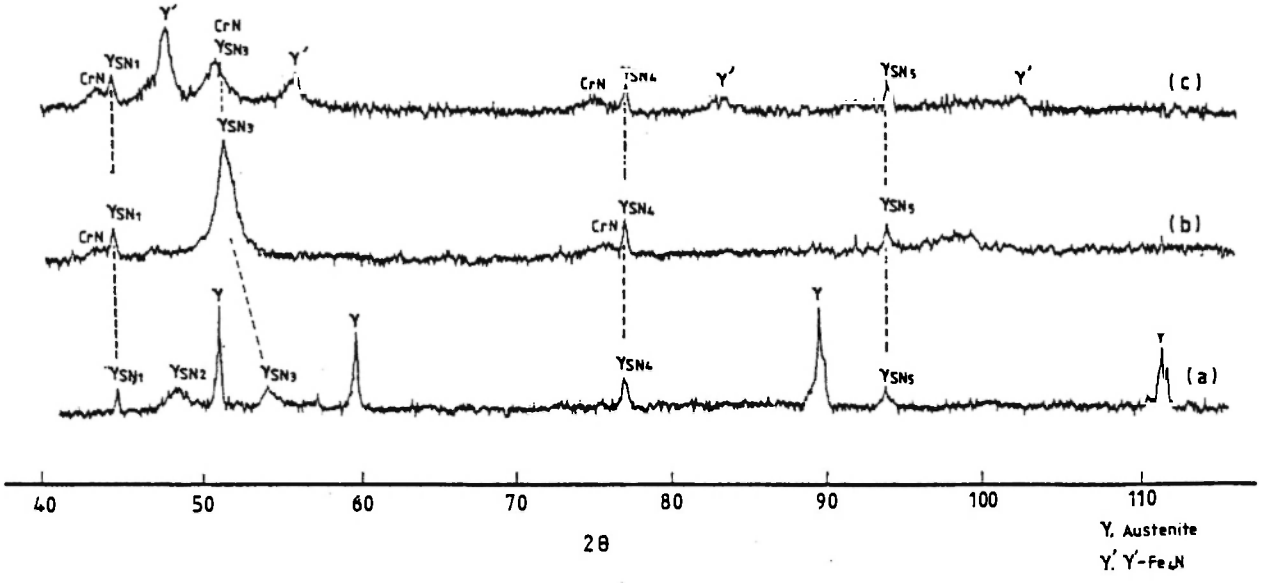

Fig. 3. X-ray diffraction patterns from the surface of SUS304 stainless steel nitrided in ammonia gas in the temperature range 693°–773°K for 26.2 ks. The patterns observed from specimens nitrided at 683°K (a), 733°K (b) and 773°K (3).

TABLE 2
Variation of lattice parameter of austenite in nitrided layer of SUS304 stainless steel nitrided at 873°K for 10.8 ks in ammonia gas and of nitrogen content in the austenite at various depth from the surface

Depth from surface g/μm	Variation of diffraction angle (2θ) of specific planes (111)	(200)	Lattice parameter calculated from 2θ of (200) plane a_0/nm	Nitrogen content in austenite estimated from lattice parameter of previous column C_N/at%
0	undetected	undetected	–	–
10	50.3	58.6	3.67	10.7
20	50.4	58.7	3.65	9.9
30	50.4	58.8	3.64	9.5
40	50.6	59.0	3.63_6	9.1
50	50.6	59.2	3.62	7.4
60	50.8	59.4	3.61	6.1
70	51.1	59.5	3.60	5.7
80	51.2	59.7	3.59	5.5
90	51.3	59.7	3.59	5.5

of austenites versus nitrogen (or carbon) content reported by a number of investigators /11–14/ with that of γ'-Fe_4N (a superlattice in austenite) referred from the ASTM card, Fig. 4 is obtained. As this γ_{SN}-phase has an fcc structure /5/, the measured lattice parameter of the phase may be put on an extended line of the linear relation plot of γ'-Fe_4N and the plots of various other austenites as shown in Fig. 4. In this way, the value of 0.406 nm in lattice parameter corresponds to a nitrogen content of about 33 atomic%. This is a remarkably high concentration for the generally known steels and again indicates that the γ_{SN}-phase consists of a nitrogen supersaturated solid solution.

3.2. *Thermogravimetric Analysis of the γ_{SN}-phase*

SUS304 stainless steel foils of 15 μm thickness nitrided at 673°K and 743°K for 32.4 and 23.4 ks respectively (i.e. almost nitrided into the γ_{SN}-phase)

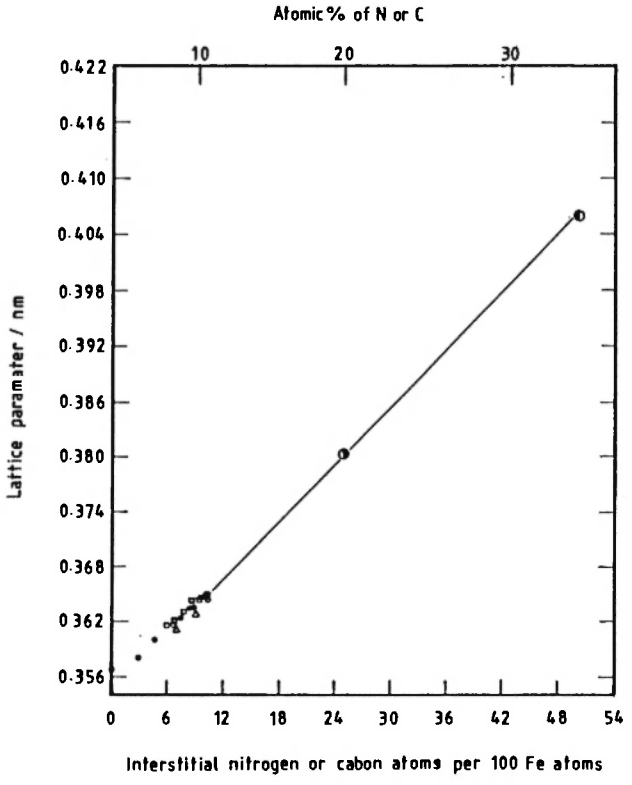

Fig. 4. Lattice parameter of austenite, γ'-Fe_4N (○) and γ_{SN} (○) as a function of nitrogen or carbon concentration reported by various investigators (● Jack /11/, Δ Bose and Hawkes /12/, □ Paranjpe *et al.* /13/, ○ Tsuchiya *et al.* /14/).

were analysed with a thermobalance from room temperature to 773°K, at various heating velocities (1/30, 1/12, 1/6, 1/3 and 5/6 deg·s^{-1}) in a nitrogen atmosphere. Typical thermograms obtained are shown in Fig. 5 (a) and (b). A marked change in the mass loss takes place within a narrow temperature range in the vicinity of 673°K for all heating velocities. The same specimen was heated by another technique, in a quartz tube under hydrogen or nitrogen atmosphere in the temperature range 773~723°K, and sampling of the exhaust was analysed by gas chromatography. A chromatogram of the specimen heated in hydrogen is shown in Fig. 6. Nitrogen was detected in the exhaust with hydrogen. This shows that the decrease in mass in Fig. 4 results in the desorption of nitrogen from the γ_{SN}-phase to a gaseous phase. Other specimens heated in nitrogen atmosphere within the same temperature range for 1.8 ks were examined by X-ray diffractometer and a typical diffraction pattern is shown in Fig. 7. Clearly, γ'-Fe_4N and CrN are detected with the co-formation of Fe_3O_4 whilst γ_{SN}-

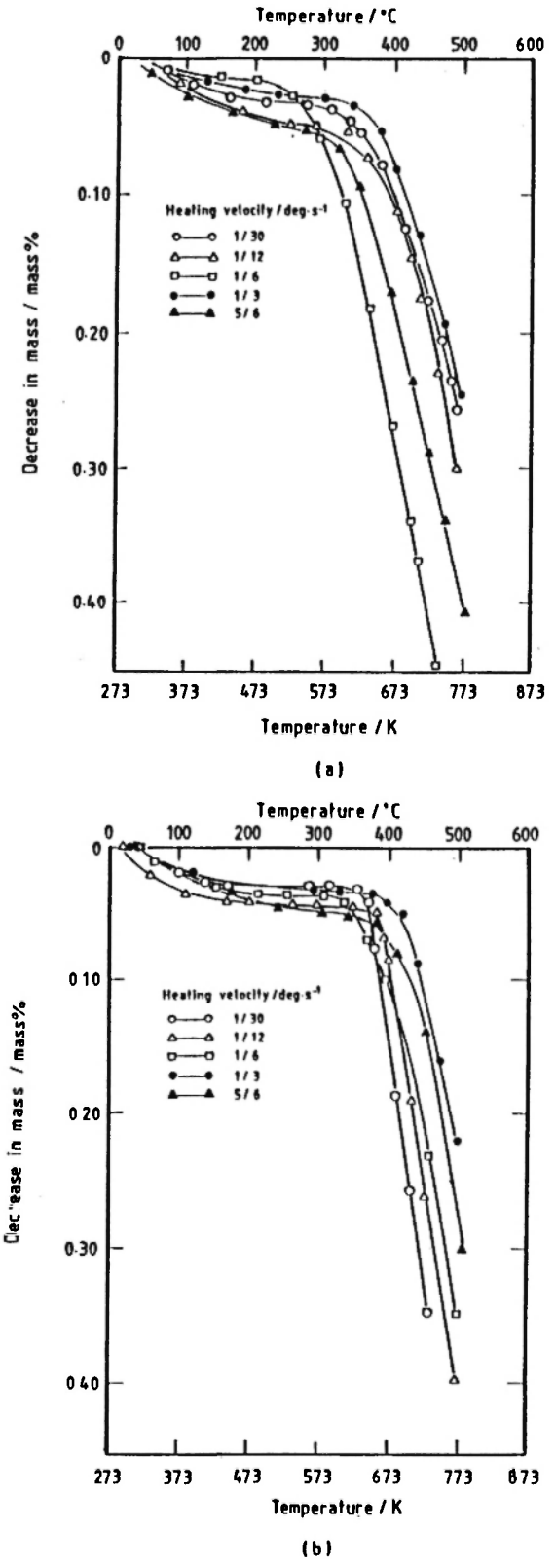

Fig. 5. Decrease of mass vs temperature in results of thermogravimetric analysis of SUS304 stainless steel specimens of 15 μm thickness, nitrided at 673°K for 32.4 ks (a) and 743°K for 23.4 ks (b), respectively.

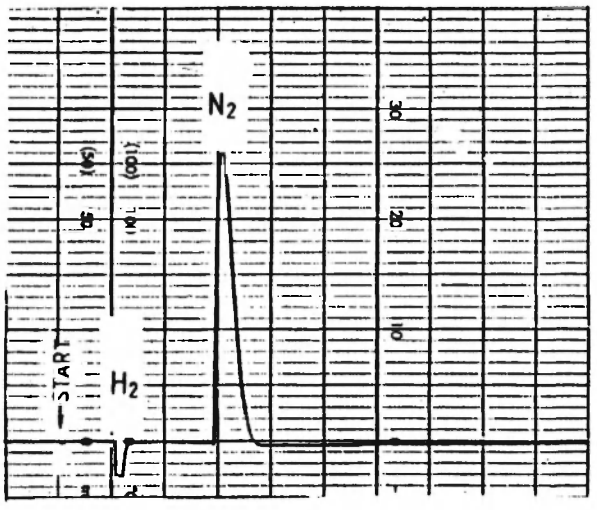

Fig. 6. Gas chromatogram of desorption gas from SUS304 steel foil nitrided at 713°K for 21.8 ks reheated under nitrogen atmosphere in temperature range 773° – 823° K.

phase disappears by this treatment. These facts prove that γ_{SN}-phase was transformed into CrN and γ'-Fe_4N [or γ'-$(Fe, Ni)_4N$] at temperatures over approximately 673°K with desorption of nitrogen. In 74Fe–18Cr–8Ni ternary alloy, the equivalent nitrogen for the formation of CrN is 18 atoms and that for γ'-$(Fe, Ni)_4N$ is 20 atoms. Thus, a sum of the equivalent nitrogen for the formation of nitrides in the alloy is about 38 atoms. From Fig. 4, a sum of about 50 nitrogen atoms is estimated in γ_{SN}-phase. When the transformation occurs in the γ_{SN}-phase some nitrogen atoms should be precipitated at the same time, so the excess nitrogen atoms resulting from the formation of nitrides described above can diffuse and transfer through the alloy surface. These nitrogen atoms react together to form nitrogen molecules on the alloy surface and then desorption of the nitrogen takes place. This reaction is represented by the equation:

$$\gamma_{SN}\text{-phase} = CrN + \gamma'\text{-}(Fe, Ni)_4N + X\underline{N}^* \quad (1)$$

$$X\underline{N}^* = X/2N_2 \quad (2)$$

where N* is the excess nitrogen precipitated in γ_{SN}-phase.

Now, our experimental results are summarized as follows, together with prior results /5/:

(1) Discontinuity of the nitriding rate takes place at approximately 723°K.

(2) Enhancement of the nitriding rate also starts at approximately 723°K.

(3) Precipitation of the blackish phase in the whitish phase begins in the range 693 –723°K.

(4) The blackish phase consists of CrN and γ'-$(Fe, Ni)_4N$ and the whitish phase consists of a nitrogen supersaturated solid solution which we have termed γ_{SN}-phase.

(5) Nitrogen content of γ_{SN}-phase obtained at 753°K is estimated to be 33 atomic % approximately from the lattice parameter measurement.

(6) Austenite formed just beneath the surface of nitrided SUS304 stainless steel has a saturated nitrogen content of about 10.7 atomic %.

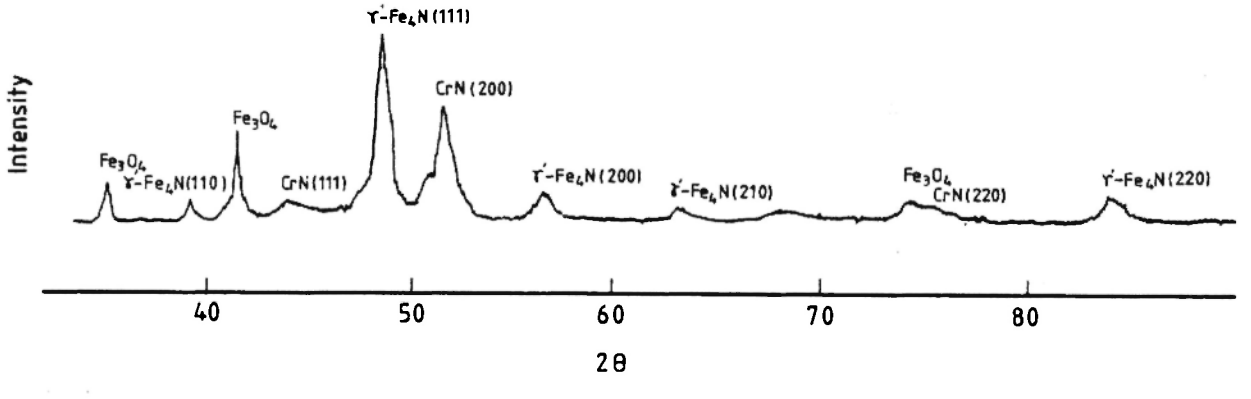

Fig. 7. X-ray, diffraction pattern of a specimen of SUS304 stainless steel foil nitrided at 713°K for 21.8 ks after being reheated in nitrogen atmosphere in temperature range 773°–823°K for 1.8 ks.

(7) γ_{SN}-phase suddenly desorps a considerable quantity of nitrogen at approximately 673°K and transforms into CrN and γ'-$(Fe, Ni)_4N$.

The above information leads to the following explanation of the irregularities in the nitriding of SUS304 stainless steel. The phenomena of enhancement and discontinuity of nitriding rate in this steel are closely connected to the precipitation process of γ_{SN}-phase formed by nitriding at approximately 733°K. From the standpoint on this concept, a kinetic model will now be considered for an understanding of the acceleration of the nitriding rate.

4. A KINETICS MODEL EXPLANATION FOR ENHANCED NITRIDING IN AUSTENITIC STAINLESS STEELS

The increase in growth rate of the nitriding layer implies that nitrogen diffusion in the alloy is accelerated. Some causes have been cited for the augmentation of such interstitial diffusion mechanisms; for example, increases of crystal imperfections and concentration gradients of diffusion atoms in alloys, thermotransports, etc. /15/.

When austenitic stainless steels are nitrided, a hardened coating is formed, in general like the previous micrographs. Now a new interpretation is needed for an understanding of the accelerated diffusion of nitrogen in SUS304 austenitic stainless steel, so any causes proposed above for the enhanced nitriding and interstitial diffusion cannot apply to this nitriding reaction. Before presentation of a model for the accelerated diffusion of nitrogen in the steel, the formation of γ_{SN}-phase should be considered in relation to the free energy-temperature diagram for the formation of chromium nitrides (Cr_2N and CrN) shown in Fig. 8 /16/. This diagram applies essentially to reactions between chromium metal and nitrogen gas at 1 atmospheric pressure as follows:

$$2\langle Cr\rangle + N_2 = 2\langle CrN\rangle \Delta G_3^\circ \quad (3)$$

$$4\langle Cr\rangle + N_2 = 2\langle Cr_2N\rangle \Delta G_4^\circ \quad (4)$$

where $\langle Cr\rangle$, $\langle CrN\rangle$ and $\langle Cr_2N\rangle$ are chromium metal and chromium nitrides as simple substances and ΔG_3° and ΔG_4° are the standard free energies of formation of CrN in Eq. (3) and Cr_2N in Eq. (4), respectively.

In the case of the nitriding of SUS304 austenitic stainless steel, chromium as an alloying element reacts

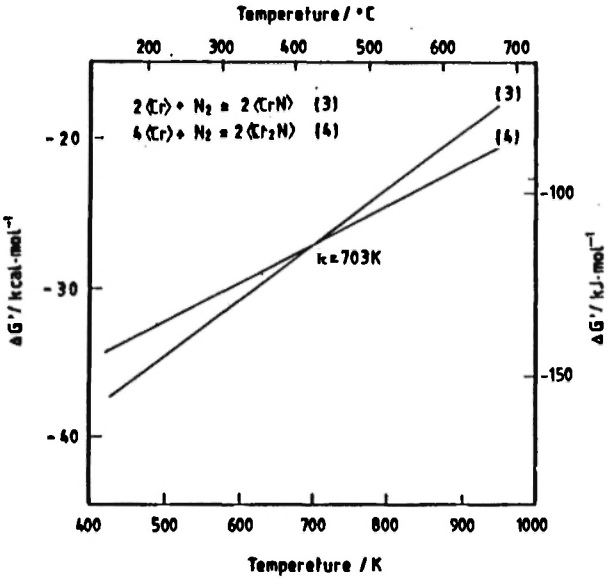

Fig. 8. Standard free energy of formation of Cr_2N and CrN as a function of temperature /16/. Tc is the intersection temperature of the $T - \Delta G^\circ$ functions of the two chromium nitrides formed by equations (3) and (4).

with nitrogen absorbed by dissociation of ammonia at the surface of the alloy and the precipitation of chromium nitrides is expected at the interface between the nitrided layer and the parent phase. These reactions are represented as:

$$(\underline{Cr}) + \underline{N} = [CrN]_{p.p}\,\Delta G_5 \quad (5)$$

$$2(\underline{Cr}) + \underline{N} = [Cr_2N]_{p.p}\,\Delta G_6 \quad (6)$$

where $(\underline{Cr})$ and $\underline{N}$ are chromium as an alloy element and a solute nitrogen atom in the alloy; $[CrN]_{p.p}$ and $[Cr_2N]_{p.p}$ are CrN and Cr_2N phases as precipitates in the nitrided layer; and ΔG_5 and ΔG_6 are changes of free energy in equations (5) and (6), respectively. In Fig. 8, as ΔG_3° in Eq. (3) and ΔG_4° in Eq. (4) intersect at approximately 703°K (Tc). Now, consider the nitriding of a steel of fixed composition under a constant pressure of ammonia, when the activity of chromium (a_{Cr}) in the alloy and the nitrogen potential (μ_N) in the atmosphere are also kept constant. This state gives other free energy functions of formation of nitrides such as ΔG_5 in Eq. (5) and ΔG_6 in Eq. (6) shifted somewhat from the position of functions ΔG_3° in Eq. (3) and ΔG_4° in Eq. (4) shown in Fig. 6. After all, functions ΔG_5 in Eq. (5) and ΔG_6 in Eq. (6) ought also to have an intersection at a tem-

perature not far from Tc, the intersection between ΔG_3° in Eq. (3) and ΔG_4° in Eq. (4). This approach develops the use of the free energy-temperature diagram of Fig. 8 in the consideration of the formation of nitrides in austenitic stainless steels during nitriding.

Precipitation in a supersaturated solid solution or transformation in a supercooled substance are often adapted to the "Stufenregel" /8/ model in terms of the step rule or hierarchy of free energy /17/. According to this theory, a nitrogen supersaturated austenite ought to firstly precipitate the Cr_2N phase in the alloy below the temperature of 703°K (Tc) and the transformation of this phase into CrN ought to take place as a subsequent step because the free energy of Cr_2N is higher than that of CrN at these temperatures. However, neither Cr_2N nor CrN precipitate in austenitic stainless steels nitrided below 703°K, only γ_{SN}-phase is formed and observed in the experimental results obtained from the present and earlier works /18/. Two reasons for this phenomenon can be postulated, one is an incoherency of lattice relations between Cr_2N (cph) and austenite (fcc) structures and the other is the relationship between nitriding temperature and mobility levels of metallic atoms in the alloy. These factors will prevent the precipitation of Cr_2N in γ_{SN}-phase. When Cr_2N cannot be precipitated, CrN will never be precipitated because of the "Stufenregel" restriction. Thus, γ_{SN}-phase only is formed and the nitrogen content in this phase becomes higher as the temperature rises, causing the ammonia to dissociate at a faster rate. At temperatures above Tc, the relation of free energy between Cr_2N and CrN is reversed as shown in Fig. 8. As CrN (fcc) has a good lattice compatibility with austenite, as summarised in Table 3, CrN will readily precipitate in γ_{SN}-phase by a reaction such as equation (1). This is confirmed experimentally in Fig. 2. But γ_{SN}-phase was still present and remained clearly in the nitrided structure at temperatures above Tc, as shown in Fig. 2. From these results, it is certain that transformation and re-formation of γ_{SN}-phase takes place in the nitrided layer simultaneously.

Lattice parameters of some substances and their lattice relationships are summarized in Table 3 for convenience.

Now a kinetics model on the enhanced nitriding mechanism in SUS304 austenitic stainless steels can be presented, with the help of the schemes illustrated in Fig. 9 (a)–(d), on the basis of the experimental results in the present work and an earlier study /5/.

In Fig. 9 (a)–(d), unit mechanisms and reactions in each stages are represented orderly as follows:

Stage (a): This step is an initial stage in which γ_{SN}-phase alone is formed by N_{ab} through the alloy surface by the following reactions:

$$NH_3 \rightarrow N_{ab} + 3/2H_2 \quad (7)$$

$$N_{ab} \rightarrow \underline{N} \quad (8)$$

$$\langle SUS304 \rangle + \underline{N} \rightarrow \gamma_{SN}\text{-phase} \quad (9)$$

TABLE 3
Lattice parameters of phases and lattice relationship between chromium nitrides and steel phases

Phase	Crystal structure	Lattice parameter (nm)
	1. LATTICE PARAMETER	
Austenite	fcc	$a_0 = 0.356 - 0.365$
Cr_2N	cph (ϵ-Ni_3N type	$a_0 = 0.4805 - 0.4759$ $c_0 = 0.4479 - 0.4438$
CrN	fcc (NaCl type)	$a = 0.4148$
γ_{SN}-phase	fcc	$a \cong 0.406$
	2. LATTICE RELATIONSHIP	
Cr_2N in α-iron	$(0001)_{Cr_2N} // (110)_{\alpha\text{-Fe}}$,	$[1\bar{1}00]_{Cr_2N} // [1\bar{1}3]_{\alpha\text{-Fe}}$ /19/
CrN in α-iron	$(100)_{CrN} // (100)_{\alpha\text{-Fe}}$,	$[010]_{CrN} // [011]_{\alpha\text{-Fe}}$ /20/ $[001]_{CrN} // [011]_{\alpha\text{-Fe}}$
CrN in γ-iron	$(100)_{CrN} // (100)_{\gamma\text{-Fe}}$	$[010]_{CrN} // [010]_{\gamma\text{-Fe}}$ /21/ $[001]_{CrN} // [100]_{\gamma\text{-Fe}}$

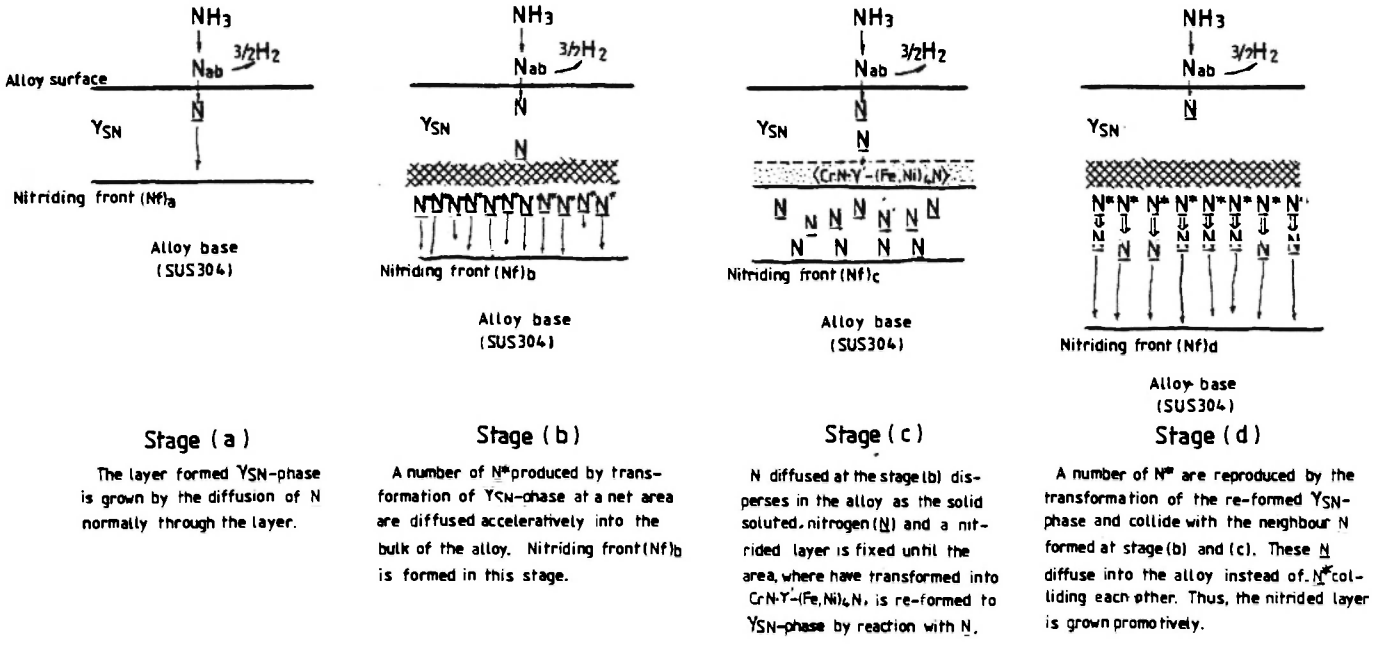

Fig. 9. Kinetics model for the enhancement mechanism of the growth of the nitrided layer in SUS304 stainless steel nitrided at a temperature above approximately 723°K.

where N_{ab} represents a nitrogen atom absorbed on the alloy surface by dissociation of ammonia gas, ⟨SUS304⟩ and N are SUS304 stainless steel and a nitrogen atom in solid solution, respectively.

Stage (b): This step marks the commencement of the enhancement of the nitriding process by the transformation of γ_{SN}-phase into an intimate mixture of CrN and γ'-$(Fe, Ni)_4N$ phase with a precipitation of nitrogen atoms at the interface between the base alloy and the nitrided layer. These reactions are as follows:

$$\gamma_{SN}\text{-phase} \rightarrow \langle \text{CrN}\,\gamma'\text{-}(Fe, Ni)_4N \rangle + x\underline{N}^* \quad (10)$$

$$x\underline{N}^* \rightarrow x\underline{N} \quad (11)$$

where ⟨CrN γ'-$(Fe, Ni)_4N$⟩ is the intimate mixture described above and $x\underline{N}^*$ is the sum of nitrogen atoms precipitated at the interface whilst reaction (10) is taking place. When reaction (10) is exothermic, $\underline{N}^*$ can be available immediately because its formation involves enthalpy of the reaction. During this stage, an extreme local concentration gradient of nitrogen content, a local temperature rise and a distortion of crystal lattice are introduced in a restricted area where reaction (10) is taking place. Reaction (11) shows that $\underline{N}^*$, activated by thermal energy, diffuses to the core of the alloy as shown in Fig. 9(b). It dissipates its energy on this path and transforms into solid solute nitrogen ($\underline{N}$) at the core.

Stage (c): During this step, γ_{SN}-phase is re-formed by the interaction of the ⟨CrN γ'-$(Fe, Ni)_4N$⟩ mixture, formed by reaction (10), with the diffused nitrogen supplied from the alloy surface by dissociation of ammonia. The reaction is:

$$\langle \text{CrN}\,\gamma'\text{-}(Fe, Ni)_4N \rangle + x\underline{N} \rightarrow \gamma_{SN}\text{-phase}_{RE} \quad (12)$$

The acceleration of nitriding is suspended until the nitrogen content in γ_{SN}-phase again reaches the original content appertaining to the phase before its transformation. In equation (12), γ_{SN}-phase_{RE} represents re-formed γ_{SN}-phase.

Stage (d): At this point γ_{SN}-phase re-formed in stage (c) is once more transformed into the intimate mixture with $x\underline{N}^*$. Then the nitriding process accelerates again. However, $\underline{N}^*$ itself will not diffuse as far as the nitriding front, as in stage (c), because precipitation of $\underline{N}^*$ takes place in the lattice interstitial positions, since nitrogen atoms already occupy solid solution positions that they filled during stage (b). This mechanism is illustrated in Fig. 9(d). The reactions are as follows:

$$\gamma_{SN}\text{-phase}_{RE} \rightarrow \langle \text{CrN } \gamma'\text{-}(Fe, Ni)_4N \rangle + x\underline{N}^* \quad (10')$$

$$x\underline{N}^* + y\underline{N} \rightarrow x'\underline{N} + y'\underline{N}^* \quad (13)$$

$$y''\underline{N}^* + z\underline{N} \rightarrow z'\underline{N} \quad (14)$$

Reactions (13) and (14) represent an exchange of energy between the activated nitrogen of $\underline{N}^*$ and the solid solution nitrogen of $\underline{N}$ in the nitrided layer. Reaction (13) is the first step in the stage and must take place at the γ_{SN}-phase$_{RE}$ transformation points. The xmol of $\underline{N}^*$, which are a high activated level, are precipitated by the progress of reaction (10') and ought to collide strongly with the ymol of $\underline{N}$ in the neighbouring lattice interstitial positions. These interstitial nitrogen atoms have then to transfer further into the alloy and, at the same time, they release most of the energy that they gained from the $x\underline{N}^*$. Thus, the y'mol of $\underline{N}^*$ produced by this mechanism ought to act against the nitrogen in solid solution in the same manner as the precipitated $\underline{N}^*$ in reaction (10') and x'mol of $\underline{N}$ which remain there until the next transformation happens. Reaction (14) is the final step. z' mol of $\underline{N}$ are distributed to a new space in the alloy and then a new nitriding front is developed. By repeating the process of stages (b), (c) and (d) in Fig. 9, the acceleration in growth rate in the nitrided layer would take place in steady state conditions.

Summarizing, the cause of the enhancement of the nitriding process in SUS304 stainless steel has been investigated and a kinetics model for understanding this phenomenon is suggested which considers the concept of "Stufenregel" in a supersaturated solid solution together with the free energy of formation-temperature diagram of chromium nitrides. The model presented in Fig. 9 shows a diffusion system resulting from a chemical reaction well known as a steady state non-equilibrium and non-linear process. So, if the enhancement of the nitriding can be explained by the kinetics model presented, it will not be necessary to describe the phenomenon in terms of diffusion theory based on statistical mechanics.

Enhanced or compelled diffusion is known under conditions of various imposed external forces /15/. However, a diffusion coefficient in an enhanced state is only $1.5 \sim 2.0$ times that in a thermally activated state. From this viewpoint, enhancement of the nitriding process in SUS304 stainless steel can be discussed from a different standpoint to the usual treatment of enhanced diffusion. In the kinetics model, Fig. 9, the activated nitrogen atoms of $\underline{N}^*$ do not diffuse to the nitriding front; all the nitrogen atoms in solid solution behave themselves just like elastic balls struck on a billiard table, and a certain amount of energy devoted to/from $\underline{N}^*$ is transported by the solid solution nitrogen atoms to the core of the alloy and dissipated through this diffusion process.

Although interstitial diffusion in metals is essentially irreversible, the kinetics of the diffusion mechanisms are described in general from the standpoint of diffusion coefficient variations based on the Arrhenius equation using the equilibrium thermodynamics functions of the activated enthalpy (ΔH^*) and entropy (ΔS^*). In the field of non-equilibrium thermodynamics, the concepts of entropy production (ΔS_i) and entropy acceleration ($-d\Delta S_i/dt$) are introduced. Considering γ_{SN}-phase transformation in the nitrided layer as shown in Fig. 9(b) and (d), it may be considered that there is a spring to gush entropy. Adding this entropy production (ΔS_i) to the activated entropy (ΔS^*) for the frequency factor in the Arrhenius equation, the enhancement of nitriding in SUS304 stainless steel can be better understood. But other approaches to these phenomena may be considered. For example, from a consideration of the instability of γ_{SN}-phase based on thermodynamic branching as suggested by Thompson /22/ or from a steady state far-from-equilibrium situation, as postulated by Prigogine /23/.

5. CONCLUSIONS

The enhancement of the nitriding process in SUS304 austenitic stainless steel has been investigated in the temperature range 673 –923°K in ammonia gas from the standpoint of the formation of chromium nitrides (Cr_2N and CrN) in the nitrided layer based on the free energy of formation-temperature diagram of these nitrides.

Observation with optical microscopy shows that precipitation of a whitish phase in the nitrided layer at about 723°K triggers an acceleration in growth rate of the layer. A discontinuity in the nitriding rate occurs at this temperature. Lattice parameter measurements by X-ray diffractometry indicate that the whitish layer formed at 753°K has an fcc structure and is a nitrogen supersaturated solid solution of approximately 33 atomic % nitrogen, called γ_{SN}-phase in this paper. The experimental results of thermo-

gravimetry for γ_{SN}-phase, of gas chromatography for sampling gas desorped from γ_{SN}-phase at elevated temperature and of X-ray diffractometry of the residue show that γ_{SN}-phase transforms into CrN and γ'-$(Fe, Ni)_4N$ at about 673°K with the simultaneous precipitation of nitrogen atoms within the phase. All the critical temperatures at which sudden changes occur in these experimental results agree substantially with the intersection temperature of the chromium nitrides free energy functions on the free energy-temperature diagram. These facts lead to the conclusion that the nitriding behaviour of SUS304 austenitic stainless steel, especially the enhanced nitriding phenomenon, is related to a tendency of chromium nitrides to form in the nitrided layer through a "Stufenregel" effect.

It is of interest to note that the formation of a nitrogen supersaturated solid solution, similar to γ_{SN}-phase in SUS304 stainless steel, is expected in an austenitic Fe–V–Ni ternary alloy, because the free energy functions of VN (fcc) and V_3N (cph) intersect at about 1550°K on their free energy-temperature diagram in an analogous way to the free energy intersection of chromium nitrides /24/.

ACKNOWLEDGEMENTS

We would like to thanks Mr. O. Nakano and Mr. H. Doi (National Research Institute for Metals) for help with the experiments. Thanks are due to Professor T. Watanabe (School of Humanities and Culture, Tokai University) for valuable discussions. And special thanks are extended to Mr. K. Ohno (Daichi Netsushori Co. Ltd.) and Mr. K. Ohhori (Sohryo Denki Kagaku Co. Ltd.).

REFERENCES

1. JONES, B.J., *Iron and Steel Inst.*, (London), Advance Copy No. 8, 169 (1937).
2. LEBRUN, J.-P., MICHEL, H. and GANTOIS, M., *Hem. Sci. Rev. Metall.*, **6**, 727 (1972).
3. EDENHOFER, B., *Harterei-tech. Mitt.*, 30, 204 (1975).
4. BILLON, B. and HENDRY, A., *Surface Eng.*, 1, 114 (1985).
5. GEMMA, K. and KAWAKAMI, M., *J. Japan, Inst. Metals*, **52**, 701 (1988).
6. GEMMA, K., KAWAKAMI, M. and UEDA, H., *Pureitingu to Kotingu*, **8**, 171 (1988).
7. GRIEVESON, P. and TURKDOGAN, E.T., *Trans. AIME*, 230, 407 (1940).
8. OSTWALD, W., *Z. Phys. Chem.*, **22**, 289 (1897).
9. YASUMARU, N. and KAMACHI, K., *J. Japan, Inst. Metals*, 50, 362 (1986).
10. ICHII, K., FUJIMURA, K. and TAKASE, T., *NETSU SHOR*, 25, 191 (1985).
11. JACK, K.H., *Proc. Roy. Soc.*, **A208**, 200 (1951).
12. BOSE, B.N. and HAWKIS, M.F., *J. Metals*, **188**, 307 (1950).
13. PARANJPE, V.G., COHEN, M., BEVER, M.B. and FLOE, C.F., *J. Metals*, **188**, 261 (1950).
14. TSUCHIYA, M., TZUMIYAMA, M. and IMAI, Y., *J. Japan, Inst. Metals*, 29, 427 (1965).
15. GUIRALGENQ, P., "Diffusion dans les Metaux", Chapitre 4, Techniques de l'ingenieur" (1978).
16. KUBASCHEWSKI, O., IVANS, E.LI. and ALCOCK, C.B., "Metallurgical Thermochemistry", Pergamon Press, England (1967).
17. CAHN, J.W., "Rapid Solidification Processing, Principles and Technology II", Claitor's Publishing Division, 24 (1980).
18. ZHANG, Z.L. and BELL, T., *Surface Eng.*, 1, 131 (1985).
19. KIKUCHI, M., NAGAKURA, S. and OKETANI, S., *Proc. ICSTIS, Suppl. Trans. ISIJ*, 11, 1216 (1971).
20. TANINO, M. and AOKI, K., *Trans. ISIJ*, **8**, 337 (1968).
21. RAMASWAMY, V. and WESI, D.R.F., *J. Iron Steel Inst.*, 208, 391 (1970).
22. THOMPSON, J.M.T., "Instabilities and Catastrophes in Science and Engineering", Chapter 5, John Wiley and Sons Ltd., England (1982).
23. PRIGOGINE, I., 5th Nobel Symposium, Sodergran, 371 (1967).
24. PANKRATZ, L.B., STUVE, J.M., POPPLETON, H.O., ODEN, L.L. and MAH, ALLA, D., Bureau of Mines Report of Investigations, RI 7585, United States (1971).